ARTICLE

OBC
www.rsc.org/obc

ESR study of spin-trapping with two glycosylated analogues of PBN able to target cell membrane lectins

Florence Chalier,* Olivier Ouari and Paul Tordo
UMR 6517, CNRS et Universités d'Aix-Marseille I et III, Laboratoire de Synthèse et Réactivité des Espèces Paramagnétiques, case 521, 13397 Marseille Cedex 20, France. E-mail: chalier@srepir1.univ-mrs.fr

Received 17th November 2003, Accepted 14th January 2004
First published as an Advance Article on the web 23rd February 2004

The spin trapping behaviour of the two galactosylated nitrones LAMPBN and TA1PBN, both of which are able to target cells through recognition by cell membrane lectins, were widely investigated on a variety of free radicals in aqueous media. The ESR spectra of the more amphiphilic nitrone, TA1PBN, were interpreted in the light of the LAMPBN trapping results. The spin adducts of nitrone TA1PBN, which may be better distributed inside the cell, were surrounded by two distinct environments due to the tensioactive organisation of the trap and gave two different ESR signals for each radical trapped.

Introduction

The combination of electron spin resonance (ESR) with spin trapping is nowadays a widely accepted and valuable tool[1] for detecting free radicals that are believed to play a role in the aetiology of various diseases.[2] One of the properties required by a spin trap[3] is a fast rate of addition of transient radicals in order to prevent them from disappearing in biological processes.[4] Furthermore, the resulting spin adducts must be persistent enough to reach and maintain an ESR detectable concentration and they must be easy to identify and to assign to the trapped free radicals. Trapping with nitrones such as DMPO and PBN (Scheme 1) leads to distinctive ESR signals of the various nitroxides produced.[5] However, *in vivo*, the interpretation of trapping studies can be hampered by the presence of impostor nitroxides produced by nucleophilic addition[6,7] or inverted spin trapping[8] or by degradation of the spin adducts.[9] Another problem is whether the trap reaches the radical formation site, which is often in the inner cell. When a low concentration of radicals is detected with ESR, it is difficult to appreciate whether the radical pathway is a minor process, or the major cause of the pathological progression.[10] The radicals detected are expected be the primary upstream radicals but they often belong to the radical reaction chain. Therefore some attempts to improve biodistribution of traps, to accelerate addition of radicals and to increase persistency of the resulting adducts have been made through substitution of DMPO and PBN.[11]

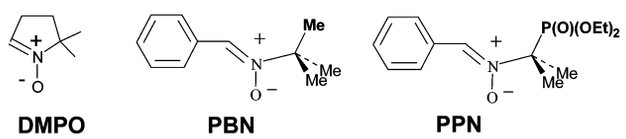

Scheme 1

We recently reported[12] the synthesis and superoxide trapping properties of the two glycosylated nitrones *N*-4-(lactobionamidomethylene) benzylidene-*N*-*tert*-butylamine *N*-oxide (LAMPBN) and diethyl-[1-methyl-1-[4-(lactobionamidomethylene)benzylidene]-zinoylethyl]phosphonate (LAMPPN) (see Scheme 2),[13] derived from nitrone PBN. Nitrone LAMPBN, like PBN, presented in phosphate buffer a very transient superoxide adduct. The superoxide adduct of nitrone LAMPPN, which differs from LAMPBN only by a β-phosphoryl group, nevertheless presented a longer half-life,

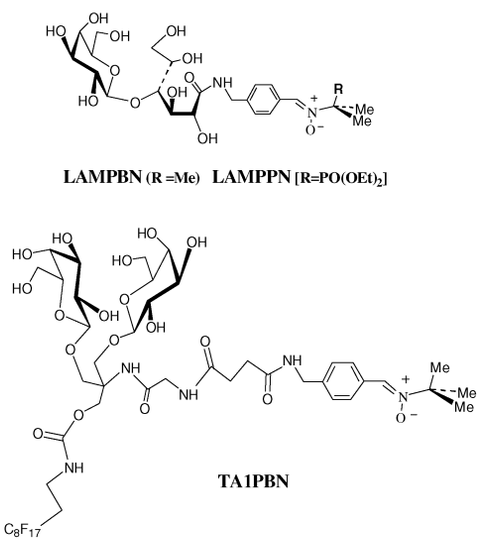

Scheme 2

as observed for nitrone PPN[14] (Scheme 1) in comparison with PBN. In any event, LAMPBN and LAMPPN had the advantage of being recognisable by the β-galactose-specific lectin KbCWL1. They could then target cells containing in their membrane this kind of galactose receptor which is known to introduce its bound glycosylated ligands into the inner cell by endocytosis. It is worthy of note that the cells of the reticuloendothelial system bear lectins that mediate the leucocyte routing in the inflammatory response and their adhesion to the inflammatory insult site,[15] and furthermore, that oxygen-centred radicals play a role in necrotic phenomena observed in chronic inflammation.[2,16] Galactose-specific lectins are also included in liver cells, such as hepatocytes[17] and macrophages (Kupffer cells),[18] and they are believed to function in the cellular translocation of glycoproteins from the blood stream for further degradation.[19] In our research on nitrone delivery *via* cell targeting and membrane crossing for diagnostic but also therapeutic applications, both nitrones LAMPBN and LAMPPN are the first members of a new series of valuable spin traps. To improve membrane crossing and protection inside biological fluids, a more complex glycosylated nitrone TA1PBN (Scheme 2) was built from PBN with a biocompatible amphiphile ligand where two hydrophilic galactosylated heads for suitable targeting are spaced out one amino acid apart from

DOI: 10.1039/b314706a

Table 1 NMR chemical shift values of the ^{13}C carbon atoms of PBN and TA1PBN in different solvents

Solvent	$E_{T(30)}$	δ_{13C} PBN	δ_{13C} TA1PBN	δ_{13C} AcTA1PBN
CCl_4	32.5	126.96		
C_6D_6	34.5	128.33		
$CDCl_3$	39.1	129.82		129.67
DMSO	45	128.53		
C_2D_5OD	51.9	133.53		
CD_3OD	55.5	134.93	134.92	134.89
D_2O	63.1	137.87		
Buffer		137.88	134.45	

a hydrophobic fluorocarbon tail.[20] This nitrone, that was recognisable by the KbCWL1 lectin,[21] has been shown to rescue complex V-deficient skin fibroblasts from apoptosis likely induced by superoxide overproduction.[22] The shape of its ESR spin adduct signals seems to be strongly dependent upon the nature of the trapped free radicals.[20] We detail herein its trapping behaviour on a wide variety of free radicals, using the trapping results obtained with the simpler nitrone LAMPBN for better interpretation.

Results and discussion

At the concentration needed for trapping studies (10–100 mM), which is more than ten times higher than the critical micelle concentration, the nitrone was organised mainly in supramolecular polydispersed systems with fluctuating sizes, from the size of a micelle up to 1 μm.[23] These systems included monobilayer vesicles and aggregates. To ascertain the location of the nitronyl function in this heterogeneous milieu, we decided to investigate the micropolarity of its surroundings through a ^{13}C NMR study. This method has already been used to locate PBN within micelles, or vesicles and microsomes.[24] The nitronyl chemical shift has shown a great sensitivity to solvent polarity and the downfield shift of the ^{13}C resonance with increasing polarity could be explained by an increasing contribution of the charge-separated canonical structure **1** with electron deficiency on the nitronyl carbon (Scheme 3).

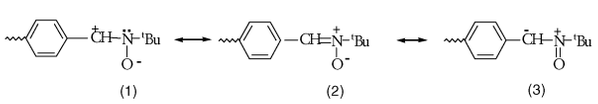

Scheme 3

Therefore the nitronyl ^{13}C chemical shifts of PBN were previously measured in several solvents (see Table 1) to establish a scale of chemical shift *versus* solvent polarity. As shown by the calibration curve in Fig. 1, the nitronyl ^{13}C chemical shift increased linearly (δ = 0.340353 × $E_{T(30)}$ + 116.243), with a reasonably good correlation coefficient r^2 equal to 0.995 and a solvent polarity parameter[25] ranging from 35 to 65. The chemical shift recorded for the TA1PBN nitronyl function in buffer disclosed the micropolarity of the microenvironment experienced by this function. When its δ (Table 1) was reported on the above plot, the corresponding polarity was $E_{T(30)}$ = 53.49 kcal mol^{-1}. However, this chemical shift recorded in buffer was a weighted, time-averaged value, since TA1PBN may be distributed between the bulk aqueous phase and the interior of the vesicles or dynamic micelles. Furthermore, due to the presence of the *para* substituent (amidomethylene) on the benzene ring, in a given environment the nitronyl $\delta^{13}C$ of TA1PBN may be slightly shifted compared to that of PBN. This electron-withdrawing group could favor the canonical structure **3** given in Scheme 3 and electron enrichment on the carbon resulted in an upfield resonance. However, nitrone AcTA1PBN[20] which differed from TA1PBN by acetyl-substitution on the hydroxyl groups of the sugar moiety, actually exhibited in CD_3OD and $CDCl_3$ (it was not soluble in water) a value of nitronyl $\delta^{13}C$ only

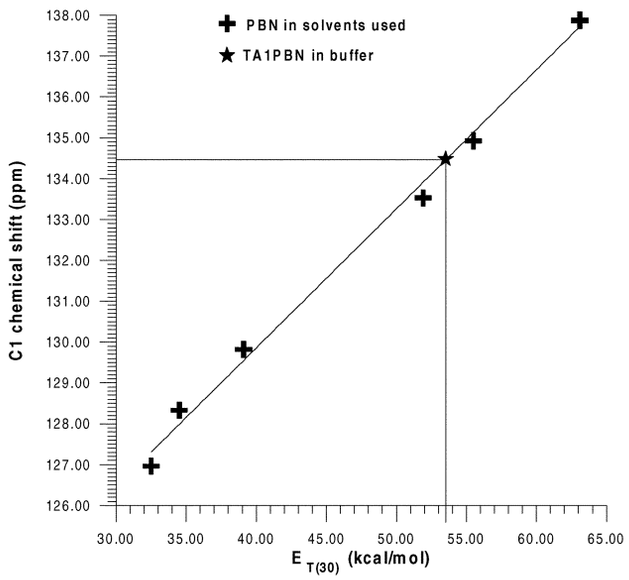

Fig. 1 Chemical shift of $^{13}C_1$ carbon atom of PBN *versus* solvent polarity parameter $E_{T(30)}$.

slightly lower than that of PBN (0.04 ≤ $\Delta\delta$ ≤ 0.15, Table 1). The similar chemical shifts of PBN and TA1PBN in CD_3OD (Table 1) and the calculated micropolarity $E_{T(30)}$ of the microenvironment experienced by the nitronyl function of TA1PBN proved nevertheless its residency in a very polar region (although less polar than water), like alcoholic surroundings. The nitronyl functions were suspected to be located mainly in the interior of the vesicles near the head group zone of the bilayer constituted of the galactosyl groups, but neither on the vesicle surface nor in the vesicle apolar core.

Spin trapping studies

Superoxide $O_2^{\bullet -}$ is often considered to be the prime radical of oxidative stress whereas the hydroxyl radical $HO^{\bullet}$ is considered to be the predominant radical contributing to injury to tissues or cells through peroxidation of their components.[26] In the radical pathway, carbon-centred species generally result from the oxidative attack of cell components. In aqueous solution, the hydroxyl spin adduct PBN-OH lasts only a few seconds[27] while the superoxide spin adduct PBN-OOH decays even more rapidly,[28] and its half-life has not been yet measured. PBN is particularly useful to trap carbon-centred radicals.[3,29] Therefore we firstly investigated hydroxyl radical trapping, then carbon centred radical trapping and finally superoxide trapping.

Trapping of the hydroxyl radical in aqueous phase. Incubation of LAMPBN with a Fenton system (2 mM hydrogen peroxide and 2 mM ferrous sulfate) and ethylenediaminetetraacetic acid (EDTA, 2 mM) in phosphate buffer (100 mM) at pH 7 led to intense ESR signals (Fig. 2a) which were satisfactorily simulated[30] assuming the presence of three various species. In the presence of metal cations, pyrroline *N*-oxides can add water to form the corresponding hydroxylamines, which are then oxidised to nitroxides.[6,31] No signal, however, was observed using either only ferrous or ferric sulfate (2 mM) and EDTA (1 mM) in phosphate buffer also containing LAMPBN, or using the Fenton system in the presence of catalase (3600 u cm^{-3}), which indicated that the hydroxyl radicals were responsible for the formation of three species giving rise to the ESR signals observed. Two of the signals had ESR parameters identical to those of PBN-OH (triplet of doublets star-plotted in Fig. 2a) and of the nitroxide ^{t}BuN(O$^{\bullet}$)H (quartet cross-plotted in Fig. 2a, A_N = A_H = 1.48 mT), both of which have been observed in ESR spectra of $HO^{\bullet}$ trapping with PBN. Nitroxide ^{t}BuN(O$^{\bullet}$)H has been shown to result from the degradation of

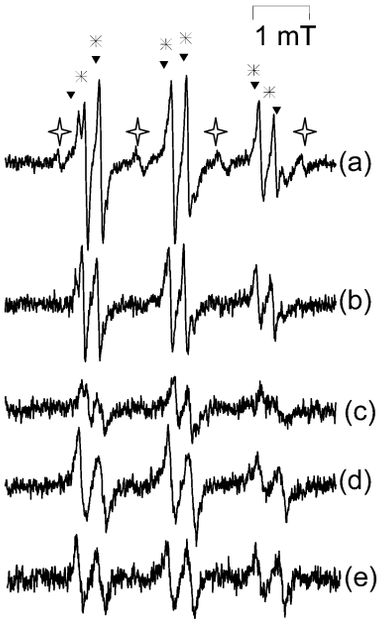

Fig. 2 Observed ESR spectra 1 min after HO$^{\bullet}$ generation with 2 mM (H_2O_2–$FeSO_4$) system in 0.1 M phosphate buffer in the presence of 0.1 M LAMPBN and 1 mM EDTA (a) at pH 7; (b) at pH 5.6; (c) at pH 8.2; (d) Like (a) but after 54 min incubation; (e) Like (a) but in the presence of 0.1 M *N-iso*-propyllactobionoamide and 0.1 M PBN instead of LAMPBN. Spectrometer settings: microwave power, 10 mW; modulation amplitude, 0.031 mT except for (e) (0.05 mT); time constant, 0.04 s; gain, 5×10^5 except for (e) (1×10^6); scan range, 10 mT and scan time, 84 s.

PBN-OH to form benzaldehyde.[32] Therefore, we assigned the first species to LAMPBN-OH (Table 1) and the second to its paramagnetic degradation product. In our experiments, nitroxide ^{t}BuN(O$^{\bullet}$)H was very transient and was not observed every time nor at every pH (Fig. 2b and 2c). Without the use of a metal chelating agent, the same signals were observed but with a weaker intensity. When using diethylenetriamine pentaacetic acid (DETAPAC) instead of EDTA or at basic pH (Fig. 2c), the third species was predominant. The third species had ESR parameters (triplet of doublets triangle-plotted in Fig. 2a, $A_N = 1.58$ mT and $A_H = 0.348$ mT), close to those of the persistent PBN-CH_2OH ($A_N = 1.61$ mT and $A_H = 0.386$ mT) and as expected its signal was observed alone (Fig. 2d) after the other two had disappeared. Assuming that the scavenging of the carbon centred radicals issued from the glycosylated moiety of LAMPBN may be responsible for this third species, trapping tests were done with PBN in the presence of the hydroxyl radicals and *N*-isopropyllactobionoamide (equimolar to nitrone) or *N*-isopropylgluconoamide. The close similarity of the resulting signals (Fig. 2e) with the spectrum of Fig. 2c proved that the lactobionoamide moiety competed with the nitronyl function to react with HO$^{\bullet}$.

At acidic pH (5.6) under the above experimental conditions, the LAMPBN-OH signal was observed for 20 min while it was seen for 10 min at pH 7 and only 5 min at basic pH (8.6). LAMPBN-OH was obtained alone by 30 s to 1 min UV photolysis (1000 W, Xe-Hg lamp) of a 10% hydrogen peroxide solution in neutral phosphate buffer containing also LAMPBN and DETAPAC, and this method of generation was used to estimate the adduct half-life at pH 7. The decay of the adduct was followed by monitoring the intensity of the third line of its ESR spectrum (Fig. 3). The decay curve was satisfactorily simulated[33] assuming a pseudo first order decay process (decay rate constant $k_d = 1.7 \pm 0.03 \times 10^2$ M^{-1} s^{-1}) and the half life was estimated at 40 s at pH 7.4. A half life of 38 s has been found for PBN-OH using similar experimental conditions but with a lower concentration of hydrogen peroxide to avoid formation of superoxide adduct.[33,34] With LAMPBN no superoxide

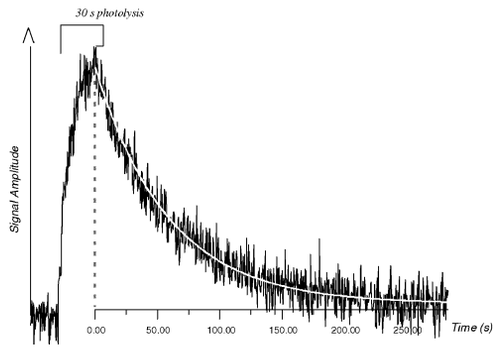

Fig. 3 Observed ESR signal amplitude curve (dark line) and simulated first order decay (white line) of LAMPBN-OH when HO$^{\bullet}$ was generated by 30 s UV-photolysis of a solution containing LAMPBN (0.1 M), H_2O_2 (10%) and DETAPAC (1 mM) in phosphate buffer (0.1 M, pH 7.) Spectrometer settings: microwave power, 10 mW; modulation amplitude, 0.09 mT; time constant, 0.08 s; gain, 8×10^5; static field, 348 mT; and scan time, 335.54 s.

adduct was observed even using hydrogen peroxide at concentrations above 10%, and at concentrations lower than 10% the signal of LAMPBN-OH was weaker and superimposed on the signal of the carbon centred radical adducts. For PBN it has been reported that the hydroxyl adduct decay could follow a second-order kinetic when the adduct concentration was higher than 2×10^{-4} mol L^{-1} and high enough to induce disproportionation. The first order simulation of the decay of LAMPBN-OH led us to conclude that under our experimental conditions this adduct did not reach a concentration high enough to induce disproportionation and that the main decay process afforded benzaldehyde and ^{t}BuN(O$^{\bullet}$)H as detected in Fenton experiments.

When TA1PBN was incubated with hydrogen peroxide and ferrous sulfate in phosphate buffer at pH 7, the strongly dissymmetric spectrum obtained (Fig. 4a) was satisfactorily simulated[30] assuming that an isotropic signal was superimposed on a preponderant anisotropic signal (93%). The ESR parameters of the two contributing species are given in Table 2 (entry 11). For the preponderant anisotropic signal the values of the extra-

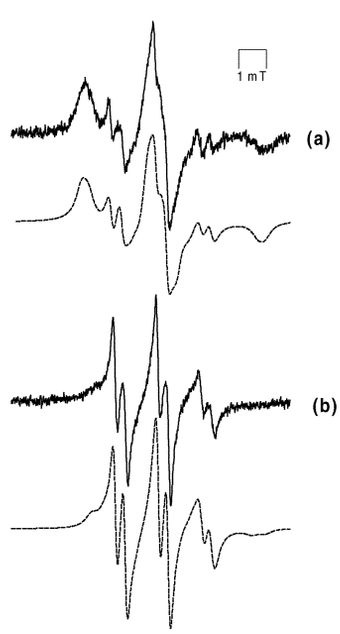

Fig. 4 Observed (full line) and simulated (dotted line) ESR spectra 1 min after hydroxyl radical generation with 2 mM (H_2O_2–$FeSO_4$) system in 0.1 M phosphate buffer in the presence of 0.1 M TA1PBN and 1 mM EDTA (a) at pH 7; (b) like (a) but after addition of 60% dioxane. Spectrometer settings: microwave power, 10 mW; modulation amplitude, (a) 0.031 mT (b) 0.06 mT; time constant, 0.04 s; gain, (a) 5×10^5 (b) 1.6×10^5; scan range, 10 mT and scan time, 84 s.

Table 2 ESR parameters of several radical adducts with PBN, LAMPBN, and TA1PBN

Species adducted, R$^{\bullet}$	R$^{\bullet}$ source	PBN-R *In buffer*	LAMPPBN-R *In buffer*	TA1PBN-R *In buffer*		TA1PBN-R *In buffer + 60% dioxane*	
		A_N A_H	A_N A_H	Isotropic A_N (%) A_H $A^{13}{}_C$	Anisotropic A_Nc ($A_{N\perp}$, $A_{N//}$) A_Hc ($A_{H\perp}$, $A_{H//}$) A_Cc ($A_{H\perp}$, $A_{H//}$)	Isotropic A_N (%) A_H	Anisotropic A_Hc ($A_{H\perp}$, $A_{H//}$) A_Hc ($A_{H\perp}$, $A_{H//}$)
$^{\bullet}$OH	Fenton System	1.54 0.27	1.55 0.270				
$^{\bullet}$OMe	H_2O_2 + DMSO + O_2/UV	1.51 0.35[a]	1.51 0.320[b]				
$^{\bullet}CH_3$	H_2O_2 + DMSO/UV	1.65 0.36[a]	1.61 0.357[b]				
$^{\bullet}$COOK	Fenton + HCOOK	1.59 0.46	1.57 0.443	1.588 (48%) 0.454	1.518 (0.796, 2.960) 0.349 (0.363, 0.321)		
	Fenton + H^{13}COOK			1.588 (48%) 0.454 1.161	1.518 (0.796, 2.960) 0.349 (0.363, 0.321) 1.212 (0.824, 0.775)		
$^{\bullet}CH_2OH$	Fenton + CH_3OH[c]	1.61 0.39	1.59 0.373	1.584 (26%) 0.374	1.461 (0.704, 2.975) 0.357 (0.400, 0.270)		
	Fenton + $^{13}CH_3OH$[c]			1.584 (26%) 0.374 0.382	1.461 (0.704, 2.975) 0.357 (0.400, 0.270) 0.319 (0.361, 0.234)		
$^{\bullet}$CH(OH)Me	Fenton + EtOH[c]	1.62 0.33	1.60 0.322	1.591 (18%) 0.330	1.476 (0.705, 3.027) 0.346 (0.380, 0.280)	1.536 (100%) 0.330	
$^{\bullet}C(OH)(Me)_2$	Fenton + *iso*-propanol[c]			1.629 (14%) 0.297	1.476 (0.689, 3.052) 0.288 (0.398, 0.070)		
$^{\bullet}C(OH)(Et)_2$	Fenton + pentan-3-ol[c]		1.60 0.297				
$^{\bullet}$CH(OH)(Pr)	Fenton + butan-1-ol[c]			1.545 (46%) 0.337	1.603 (1.038, 2.734) 0.262 (0.394, 0)	1.529 (100%) 0.320	
$^{\bullet}$CH(OH)(Pt)	Fenton + hexan-1-ol[c]			1.631 (13%) 0.279	1.447 (0.650, 3.041) 0.333 (0.367, 0.267)	1.530 (100%) 0.311	
Alkyl or alkoxyl adduct	Fenton and glycosylated moiety	1.59 0.34	1.58 0.34	1.601 (7%) 0.378	1.575 (0.784, 3.157) 0.328 (0.367, 0.247)	1.551 (32%) 0.352	1.515 (0.838, 2.874) 0.353 (0.288, 0.482)

[a] 1% DMSO. [b] 10% DMSO. [c] 10% alcohol.

polated isotropic coupling constants A_Nc and A_Hc were determined from the diagonal tensors values $A_{i\perp}$ and $A_{i//}$ following eqn. 1. The values of A_H and A_Hc of hydrogen coupling sug-

$$A_i c = 1/3\ A_{i//} + 2/3\ A_{i\perp} \qquad (1)$$

gested that both signals (isotropic and anisotropic) did not result from the direct scavenging of radicals HO$^\bullet$ and must be assigned to some carbon centred radical adducts. Furthermore, compared with the A_N values of the PBN-CH_2(OH) adduct in several solvents,[5] the A_Nc value of the anisotropic signal showed that its corresponding aminoxyl functions could be in an alcoholic or glycosidic environment. Since the constraint of the rotational motion of the aminoxyl part and the viscosity of the aminoxyl surroundings are closely correlated, we can assume that these aminoxyl functions were sequestered inside the vesicles formed by TA1PBN. The aminoxyl functions giving rise to the isotropic signal could be located outside the vesicles or at their surfaces. Assuming that the galactosylated moiety of TA1PBN, which was encountered firstly by the hydroxyl radicals, competed with the nitronyl function for HO$^\bullet$ trapping, the strongly anisotropic signal may be assigned to a condensation product, being part of the vesicle, of two (as a minimum) constitutive nitrone molecules. The dimer given in Scheme 4 is the product obtained when the HO$^\bullet$ radical attacks the primary alcohol function of the galactosylated chain when this radical is immediately trapped. However, the radicals from the sugar moiety may also degrade to aldehydes or ketones.[35] These compounds may further react with hydrogen peroxide and therefore they may be cut in fragments[36] that would be trapped inside or outside the vesicle. We added 60% dioxane to the sample to break the molecular organisation and presumably the interactions of the nitroxide with its surroundings that could hamper its free motion. The spectrum (Fig. 4b) exhibited a more symmetrical shape, however, its simulation showed that the isotropic signal was again superimposed to a great extent on the anisotropic signal (68%). The values of A_H and A_N coupling of the isotropic signal (Table 2 entry 11) were compared with those of the isotropic signal of the dioxane adduct with TA1PBN obtained singly when radical HO$^\bullet$ was generated in a milieu containing 60% of dioxane in buffer already. From its different ESR parameters (A_N = 1.512 mT and A_H = 0.290 mT) we could assume that it was not implicated in the previous spectrum. Thus, the species responsible for the more isotropic features were nitroxides released from the vesicles. They may be either the dimer species or adducts of the fragments arising from oxidation of the sugar moiety. The species with strong immobilisation of the aminoxyl function exhibited slightly different parameters when compared with experiments solely in the aqueous phase (Table 2 entry 11), however, the A_Nc could be induced by a modification of the polarity in the aggregates that were then swollen with dioxane. This species may be assigned to polymer molecules.

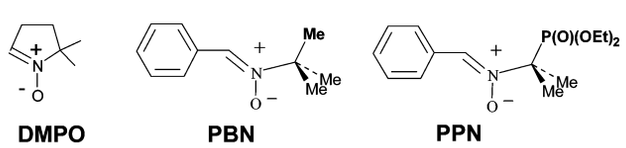

Scheme 1

Trapping of the carbon centred radicals in aqueous phase. Carbon centred radicals $^\bullet CO_2Na$ and $^\bullet CRR'(OH)$ were obtained respectively after hydrogen abstraction by the hydroxyl radicals from formate and several alcohols such as methanol, ethanol, *iso*-propanol, *n*-butanol, pentan-3-ol and *n*-hexanol in 10% concentration in phosphate aqueous buffer. Using LAMPBN the resulting trapping species exhibited ESR parameters close to those of the PBN adducts (see Table 2) with the biggest A_N for the most polar radical $^\bullet CO_2Na$ and intense and persistent signals for short chain alcohols (Figs. 5a and b).

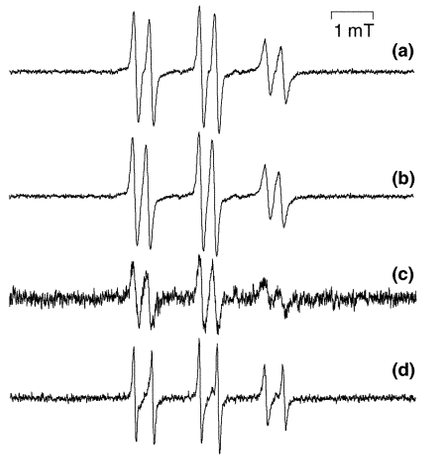

Fig. 5 Observed ESR spectra after carbon centred radical generation with 2 mM (H_2O_2–$FeSO_4$) system in 0.1 M phosphate buffer with 1 mM DETAPAC at pH 7 in the presence of 0.1 M LAMPBN and (a) 10% methanol; (b) 10% ethanol; (c) 10% *n*-pentanol; (d) 0.2 M sodium formate. Spectrometer settings: microwave power, 10 mW; modulation amplitude, 0.01 mT except for (c) (0.05 mT); time constant, 0.08 s; gain, 2×10^5 except for (c) (1×10^6); scan range, 15 mT and scan time, 84 s.

The signal obtained from pentan-3-ol was less intense (Fig. 5c), and its A_H was smaller. This can be explained by the bigger steric hindrance of the trapped radical $^\bullet C(OH)Et_2$.

When using TA1PBN the resulting spectra strongly depended on the nature of the trapped radical (Fig. 6). Two signals were observed in each spectrum but in various ratios. One was very anisotropic and presumably the interactions of the nitroxide function with its surroundings reduced its free motion. The other signal indicated less ordering (and is classed herein below as an isotropic signal). When radical $^\bullet CH_2OH$ was

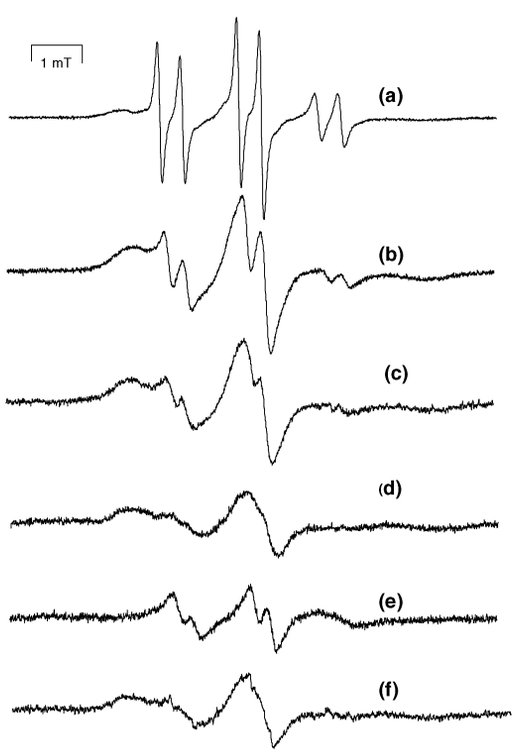

Fig. 6 Observed ESR spectra 1 min after carbon centred radical generation with 2 mM (H_2O_2–$FeSO_4$) system in 0.1 M phosphate buffer at pH 7 in the presence of 0.1 M TA1PBN, 1 mM EDTA and (a) 0.2 M potassium formate;(b) 10% methanol; (c) 10% ethanol; (d) 10% *iso*-propanol; (e) 10% butan-1-ol; (f) 10% hexan-1-ol. Spectrometer settings: microwave power, 10 mW; modulation amplitude, (a) 0.05 mT, except for (d) and (f) (0.09 mT); time constant, 0.04 s; gain, 2×10^5 except for d and f (8×10^5); scan range, 10 mT and scan time, 84 s.

generated the most strongly immobilised nitroxide was predominant. When the radical $^{\bullet}CO_2Na$ was generated, the spectrum was mainly constituted of the isotropic signal of the less strongly immobilised nitroxide.

Methanol and formate labelled with ^{13}C isotopes were used to assign the signals without any doubt. Similar superimposition of two nitroxide signals was observed (Figs. 7b and 7d). However the shape of the both signals in each spectrum changed : the isotropic triplet of doublets became a ten line signal and the anisotropic signal became broader. A new coupling of the free electron was undoubtedly involved in this change and furthermore, the ratio of the anisotropic signal to the isotropic signal was reduced when dioxane was added in the ESR-tested samples to break the vesicle organisation (Fig. 7e). Thus the two signals in each spectrum belonged to the same adduct TA1PBN-R but the aminoxyl functions resided in two different micro-surroundings and the trapped radicals were proved to be the ^{13}C centred radicals obtained by hydrogen abstraction of the methanol or the acid used. When using another alcohol we also added dioxane to the samples and the proportion of the isotropic signal increased in conjunction with the disappearance of the anisotropic signal (Fig. 8). When up to 60% of dioxane was added the spectra presented generally only the isotropic signal (see Table 2). A similar conclusion could be reached about the belonging to only one adduct TA1PBN-CRR′(OH), of the two kinds of signals in the spectra (a), (c) and (e) in Fig. 8.

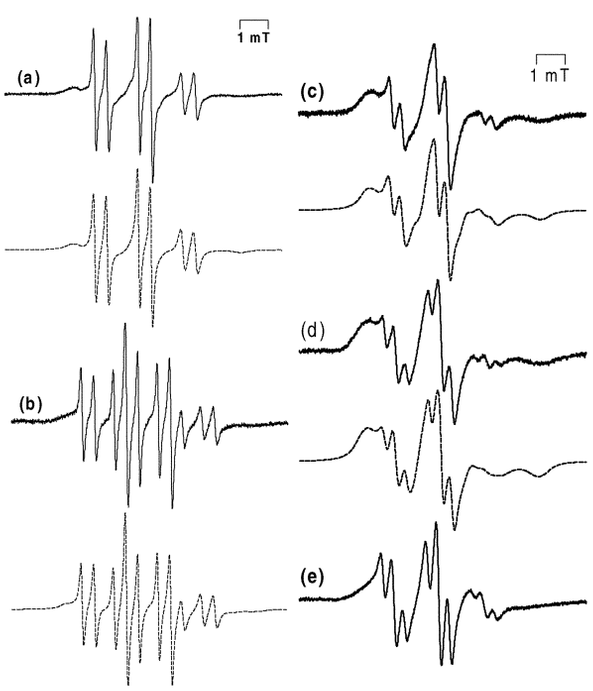

Fig. 7 Observed (full line) and simulated (dotted line) ESR spectra 1 min after carbon centred radical generation with 2 mM (H_2O_2–$FeSO_4$) system in 0.1 M phosphate buffer at pH 7 in the presence of 0.1 M TA1PBN, 1 mM EDTA and (a) 0.2 M potassium formate; (b) like (a) but $^{13}COOK$ was used; (c) 10% methanol; (d) like (c) but $^{13}CH_3OH$ was used; (e) like (d) but after addition of 20% dioxane. Spectrometer settings: microwave power, 10 mW; modulation amplitude, 0.05 mT; time constant, 0.04 s; gain, 2×10^5 scan range, 10 mT and scan time, 84 s.

According to simulation of spectra obtained from short chain alcohols (methanol to propanol) with the ROKI program, the proportion of the anisotropic signal was high and increased with the size of the carbon centred radical $^{\bullet}$CRR′(OH) trapped (Fig. 6 and 8a and Table 2). This ESR anisotropic signal could be assigned to the nitroxide TA1PBN-CRR′(OH) incorporated inside a vesicle while the isotropic signal could be assigned to this nitroxide located either outside the

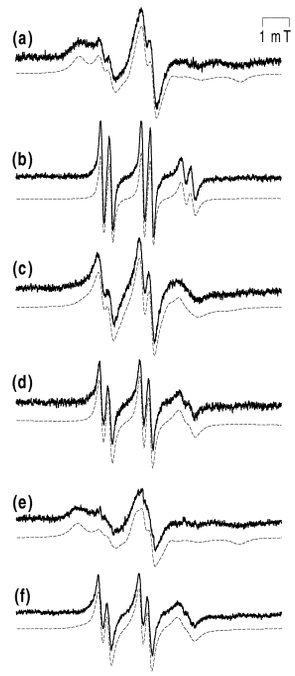

Fig. 8 Observed (full line) and simulated (dotted line) ESR spectra after carbon centred radical generation with 2 mM (H_2O_2–$FeSO_4$) system in 0.1 M phosphate buffer at pH 7 in the presence of 0.1 M TA1PBN, 1 mM EDTA and (a) 10% ethanol; (b) like (a) but after addition of 60% dioxane; (c) 10% *n*-butanol; (d) like (c) but after addition of 60% dioxane; (e) 10% *n*-hexanol; (f) like (e) but after addition of 60% dioxane. Spectrometer settings: microwave power, 10 mW; modulation amplitude, 0.05 mT except for (e) and (f) (0.09 mT); time constant, 0.04 s; gain, 5×10^5 except for (e) and (f) (8×10^5); scan range, 10 mT and scan time, 84 s.

vesicle or on its surface. The more lipophilic the radical $^{\bullet}$CRR′(OH) was, the easier it penetrated the vesicle lipophilic milieu and the higher the proportion of the anisotropic signal it was. As the A_N value of the nitroxide is a function of the electron density on nitrogen, the difference between the A_N value of the isotropic signal and the lower A_{Nc} value of the anisotropic signal revealed the apolar microenvironment of the aminoxyl function when incorporated inside a vesicle. Compared with the A_N values of the PBN-CH_2(OH) and PBN-CHMe(OH) adducts in different solvents,[5] the A_{Nc} values of the anisotropic signals proved the residency the aminoxyl function in an alkylated vesicle region, presumably in the vesicle apolar core.

The results observed with long chain alcohols proved two different effects. If *n*-hexanol was cotensioactive, *n*-butanol was detergent for tensioactive aggregation. Insertion of *n*-hexanol or $^{\bullet}CH(OH)(C_5H_{11})$ molecules in a vesicle did not break the vesicle organisation, and, as disclosed by the coupling constant A_{Nc} value which was smaller than those of the TA1PBN-CH(OH)Me adduct, it just decreased the polarity experienced by the incorporated nitroxide function. On the other hand, in the presence of *n*-butanol, the proportion of the anisotropic signal was particularly small and this showed that the insertion of *n*-butanol in the vesicles made them break up. The A_Nc value showed that the residual vesicles were swollen with water. The release of the TA1PBN molecules in the aqueous milieu was confirmed by the A_N parameter presented by the isotropic signal which was lower than that estimated when another alcohol was used, and which highlighted more lipophilic surroundings of the corresponding nitroxide function.

Trapping of superoxide in aqueous phase. We previously reported the successful behaviour of LAMPBN in trapping superoxide.[12] We tested whether TA1PBN could trap superoxide in aqueous media but generation of superoxide in 0.1 M phosphate buffer by the [xanthine oxidase–hypoxanthine]

system in the presence of the nitrone did not lead to any ESR signal at room temperature. However, this result did not prove either that TA1PBN was inefficient to trap superoxide or that its superoxide adduct was more transient than those of PBN. Since the nitronyl function is mainly encapsulated inside the vesicle, the two conjugated issues of a slow diffusion of the polar radical toward the trapping functions and of a weak persistency of the resulting adduct may explain such an ESR silent result in the aqueous phase. It is advisable not to disregard the potentiality of intracellular trapping of the oxygenated radicals since TA1PBN has been shown to lower the SOD induction of complex V-deficient skin fibroblasts[22] and since the glycosylated groups may be lost during membrane crossing.

Conclusion

Nitrones LAMPBN and TA1PBN that could be efficiently recognised by galactose specific yeast lectins through a glycosylated moiety can scavenge free radicals. As for the LAMPBN-OOH adduct, the formation and persistence of LAMPBN-OH is strongly pH-dependent with a preference for an acidic pH. However, at physiological pH the spin adducts are short lived. We have shown that carbon-centred radicals are formed and presumably result from the attack of the $^{\bullet}OH$ radicals on the lactobionamide moiety. However, the signals of the corresponding spin adducts do not hamper the identification of LAMPBN-OH. The trapping of carbon centred radicals leads only to the corresponding, very persistent adducts. Therefore LAMPBN is not a very good diagnostic tool for the study of the oxygen centred radicals involvement in pathological situations, but it could be used to trap some carbon centred radicals which are secondary products formed during the oxidative stress process. When nitrone TA1PBN is used in aqueous phase at concentrations needed for spin trapping and visualisation by ESR, the nitronyl function is mainly encapsulated in the vesicles, and is likely to be difficult to reach by the polar superoxide radical and by the hydroxyl radical which react mainly with the glycosylated moiety at the vesicle surface. However, in phosphate buffer, TA1PBN trapped the carbon centred radicals easily and the rotational motion of the aminoxyl function of the corresponding spin adducts was restricted in the vesicle organisation. Although the superoxide adduct signal was not observed by ESR in aqueous phase where TA1PBN aggregates in vesicles, in other surroundings without such aggregation of the nitrone, superoxide trapping may occur. Furthermore biological assays have suggested that this nitrone has a protective antioxidant effect against superoxide overproduction,[22] and the pharmacologic potential of nitrones as therapeutics in the treatment of neurodegenarative diseases has not been correlated to their spin trapping activities.[37] Therefore TA1PBN can be considered as a potential candidate for radical chain breaking in pathologies where oxidative stress operates as a major etiological component.

Experimental

Xanthine oxidase (from cow milk, phosphate free) and superoxide dismutase (from bovine erythrocyte) were obtained from Bœringer Mannheim Biochemica Co. Catalase (from bovine liver, 2000–5000 u mg^{-1}) and all chemicals were purchased from Sigma Chemical Co. Distilled water for the aqueous solution or buffers (0.1 M phosphate solution of KH_2PO_4 and Na_2HPO_4) were stirred before use for 6 h in the presence of a sodium iminodiacetate chelating resin (4.10^{-2} g cm^{-3}) to remove trace metal impurities. ESR spectra were mainly recorded at room temperature on a Bruker ESP 300 ESR spectrometer at 9.5 GHz (X-band) using 100 kHz field modulation and equipped with a NMR gaussmeter for magnetic field calibration. An HP 5350B microwave frequency counter was used for the determination of Landé *g* factors.

Spin-trapping of the hydroxyl radical generated by a Fenton system

A Fenton system including H_2O_2 (2 mM), DETAPAC or EDTA (2 mM) and $FeSO_4$ (2 mM) in phosphate buffer (100 mM) was used in the presence of nitrone (0.1M). The first spectra of each experiment series were recorded 1 min after addition of the last reagent ($FeSO_4$). To inhibit the formation of the hydroxyl adduct, 650 u cm^{-3} catalase was added before $FeSO_4$.

Spin-trapping of the hydroxyl radical generated by H_2O_2 photolysis

A solution in phosphate buffer (0.1 M) at pH 7 of either 1% or 10% H_2O_2, containing also 1 mM DTPA and 0.1 M nitrone was photolysed for 1 min or 30 s with a 1000 W xenon-mercury Oriel lamp. The first spectrum of each experiment series was recorded instantaneously after photolysis.

Spin-trapping of carbon centred radicals generated by action of the hydroxyl radical on alcohol or formate

The $HO^{\bullet}$ radical was generated either by a Fenton system in the presence of nitrone (0.1 M) and alcohol (10%) or formate (0.2 M) in phosphate buffer (0.1 M) at pH 7. The first spectrum of each experiment series was recorded 1 min after reagent mixing.

Spin-trapping of superoxide generated by the (xanthine oxidase–oxygen–hypoxanthine) system

The $O_2^{-\bullet}$ radicals were generated by HX (0.4 mM), and XO (0.4 or 0.04 u cm^{-3}) in the presence of nitrone (0.1 M) and DETAPAC (1 mM), in phosphate buffer (0.1 M) at various pHs (5.6, 7 and 8.2). The first ESR recording was performed 60 s after enzyme addition.

ESR simulation

The ROKI program[30] simulates isotropic signals with either a constant line-width when the tumbling rate is very rapid or with variable line-widths when the anisotropic iterations are not averaged to zero while the tumbling rate is sufficiently rapid for the line positions to correspond to those of the completely averaged spectrum. We used this latter option for simulation of the isotropic signals of the TA1PBN adducts that exhibited two broader highest-field lines. The line-width W of each hyperfine component followed the equation 2 where coefficients α, β and γ adjusted by the program depend on the anisotropies of the g factor and of the hyperfine splitting and on the mean tumbling rate. Parameters β and γ go to zero as this rate increases. In this equation M_N is the magnetic quantum number for the nitrogen atom. When the highest-field line is broader ($M_N = -1$) than the lowest-field line, the β value is negative.

$$W = \alpha + \beta M_N + \gamma M_N^2 \qquad (2)$$

The ROKI program simulated the anisotropic signal of the TA1PBN adducts (slowly tumbling nitroxide) through eight or ten adjusted parallel or perpendicular features: g, $A_{N//}$, $A_{N\perp}$, $A_{P//}$, $A_{P\perp}$, and $A_{H//}$, $A_{H\perp}$, and $A_{C//}$, $A_{C\perp}$ if ^{13}C was used. The g factor, phosphorus, nitrogen, ^{13}C carbon and hydrogen hyperfine matrixes were assumed to be parallel. The effect of residual motion (typically the parallel components are very broad and shifted to the high field region) was taken into account by introduction of a hyperfine dependent line-width tensor, where M_N is the magnetic quantum number for the nitrogen atom (eqns. 3 and 4)

$$W_{//}^2 = \alpha_{//} + \beta_{//} M_N + \gamma_{//} M_N^2 \qquad (3)$$

$$W_{\perp}^2 = \alpha_{\perp} + \beta_{\perp} M_N + \gamma_{\perp} M_N^2 \qquad (4)$$

and where axial symmetry is assumed. The orientation dependence is given by eqn. 5. To limit the number of line-width parameters, the $\beta_{//}$, $\gamma_{//}$ and $\beta_{\perp}$, $\gamma_{\perp}$ tensor elements were replaced by isotropic constants β and $\gamma_{\perp}$ adjusted by the curve fitting procedure. The line-shape function was considered Lorentzian. For each spectrum all tensorial elements were adjusted from several parameter sets by combining iteration and least square deviation between experimental and computed spectra. The optimised parameter set was obtained after convergence. The iterations trapped in local minima were recognised by significantly larger least square errors.

$$W^2(\theta) = W_{\perp}^2\sin^2(\theta) + W_{//}^2\cos^2(\theta) \qquad (5)$$

Acknowledgements

The authors thank Dr Antal Rockenbauer (Chemical Research Center, Institute for Chemistry, Budapest, Hungary) for providing the ROKI program facilities and helpful discussions about ESR spectra simulations. The authors would also like to thank Professor Roger Bonaly[21] and Professor Bernard Pucci.[23]

References

1 P. J. Thornalley, *Life Chem. Rep.*, 1986, **4**, 57–112; E. Finkelstein, G. M. Rosen and E. J. Rauckman, *Arch. Biochem. Biophys.*, 1980, **200**, 1–16; G. M. Rosen and E. Finkelstein, *Adv. Free Radical Biol. Med.*, 1985, **1**, 345–375.
2 C. E. Cross, B. Halliwell, E. T. Borish, W. A. Pryor, B. N. Ames, R. L. Saul, J. M. McCord and D. Harman, *Ann. Intern. Med.*, 1987, **107**, 526–545.
3 J. A. DeGray and R. P. Mason, *Biological spin trapping, in Electron Spin Resonance*, eds. N. M. Atherton, M. J. Davies and B. C. Gilbert, Athenaeum Press, Ltd., Cambridge, 1994, vol. 14, p. 246–301.
4 M. C. Krishna, D. A. Grahame, A. Samuni, J. B. Mitchell and A. Russo, *Proc. Natl. Acad. Sci. USA*, 1992, **89**, 5537–5541; M. C. Krishna, A. Russo, J. B. Mitchell, S. Goldstein, H. Dafni and A. Samuni, *J. Biol. Chem.*, 1996, **271**, 26026–26031.
5 G. R. Buettner, *Free Radical Biol. Med*, 1987, **3**, 259–303.
6 P. M. Hanna, W. Chamulitrat and R. P. Mason, *Arch. Biochem. Biophys.*, 1992, **296**, 640–644.
7 A. R. Forrester and S. P. Hepburn, *J. Chem. Soc. C*, 1971, **4**, 701–703; M. J. Davies, B. C. Gilbert, J. K. Stell and A. C. Whitwood, *J. Chem. Soc., Perkin Trans. 2*, 1992, 333–335.
8 L. Eberson, J. Lind and G. Merenvi, *J. Chem. Soc., Perkin Trans. 2*, 1994, 1181–1188; V. E. Zubarev and O. Brede, *J. Chem. Soc., Perkin Trans. 2*, 1994, 1821–1828; H. Chandra and M. C. R. Symons, *J. Chem. Soc., Chem. Commun.*, 1986, 1301–1302.
9 E. Finkelstein, G. M. Rosen, E. J. Rauckman and J. Paxton, *Mol. Pharmacol.*, 1979, **16**, 676–685; G. R. Buettner, *Free Radical Res. Commun.*, 1993, **19**, 579–587.
10 M. J. Perkins, *Adv. Phys. Org. Chem.*, 1980, **17**, 1–64.
11 P. Tordo, *Electron Paramagnetic Resonance*, eds. N. M Atherton, M. J. Davies and B. C. Gilbert, *The Royal Society of Chemistry*, Cambridge, UK, 1998, vol 16, p. 116–144; C. V. Coulter, G. F. Kelso, T.-K. Lin, R. A. J. Smith and M. P. Murphy, *Free Radical Biol. Med.*, 2000, **28**, 1547–1554; P. Arya, *Heterocycles*, 1996, **43**, 397–407.
12 O. Ouari, F. Chalier, R. Bonaly, B. Pucci and P. Tordo, *J. Chem. Soc., Perkin Trans. 2*, 1998, 2299–2307.
13 The abbreviated names of these nitrones refer to that of PBN, (usually named α-phenyl-*N*-*tert*-butylnitrone although its true name is *N*-benzylidene-*tert*-butylamine *N*-oxide) and that of PPN a α-phenyl phosphorylated nitrone.
14 A. Zeghdaoui, B. Tuccio, J.-P. Finet, V. Cerri and P. Tordo, *J. Chem. Soc., Perkin Trans. 2*, 1995, **12**, 2087–2089; A. Zeghdaoui, B. Tuccio, J.-P. Finet, V. Cerri, P. Tordo, *FP N°* P. V. 9502598/1995 (application for extension PCT FR. 96/00353); B. Tuccio, A. Zeghdaoui, J.-P. Finet, V. Cerri and P. Tordo, *Res. Chem. Intermed.*, 1996, **2**, 393–404.
15 A. Lasky, *Annu. Rev. Biochem.*, 1995, **64**, 113–139.
16 K. C. Bhuyan and D. K. Bhuyan, *Curr. Eye Res.*, 1984, **3**, 67–81; B. Halliwell, J. M. C. Gutteridge, *Free Radicals in Biology and Medicine*, eds. B. Halliwell and J. M. C. Gutteridge, Clarendon Press, Oxford, 1989, Chapter 8, p. 346 and p. 423–427.
17 Y. C. Lee and R. T. Lee, *Acc. Chem. Res.*, 1995, **28**, 321–327; R. L. Hudgin, E. W. Pricer, G. Aswell, R. J. Stocker and A. G. Morell, *J. Biol. Chem.*, 1974, **249**, 5536–5543.
18 P. H. Roos, H.-J. Hartman, J. Schlepper-Schäfer, H. Kolb and V. Kolb-Bachofen, *Biochem. Biophys. Acta*, 1985, **847**, 115–121.
19 N. Sharon and H. Lis, *Sciences*, 1989, **246**, 227–234; A. Morell, G. Gregoriadis, I. H. Scheinberg, J. Hickman and G. Ashwell, *J. Biol. Chem.*, 1971, **246**, 1461–1467.
20 O. Ouari, A. Polidori, B. Pucci, P. Tordo and F. Chalier, *J. Org. Chem.*, 1999, **64**, 3554–3556.
21 Aggregation of the yeast *Kluyveromyces bulgaricus* involves a galactose specific lectin Kb CWL1. When lectins are eliminated from cell membranes, the yeast cells are afforded in suspension but are no longer flocculent. If the separated lectins are mixed with these suspensions, the cells' ability to aggregate can be restored unless the lectins are previously incubated with an agonist such as glycosidic derivatives. The agonist concentration (ICF) which is needed to inhibit this reflocculation is a measure of the agonist affinity for the lectin Kb CWL1. R. Bonaly from the laboratory of *Biochimie Microbienne (Université Henry Poincaré Nancy I, Faculté de Pharmacie, 5 rue Albert Lebrun, B. P. 403, 54001 Nancy Cedex, France.)* evaluated the ICF of TA1PBN to 1.25 mM when that of galactose was 3.12 mM. Thus the nitrone TA1PBN concentration which inhibits the reflocculation is lower than that of free galactose. Therefore its affinity for *Kluyveromyces bulgaricus* yeast lectins can be considered higher than that of free galactose.
22 V. Geromel, N. Kadhom, I. Cebalos-Picot, O. Ouari, A. Polidori, A. Munnich, A. Rötig and P. Rustin, *Human Mol. Genet.*, 2001, **10**, 1221–1223.
23 Results obtained from electronic microscope photographs with phase contrast optic (negative coloration) of a buffer solution of TA1PBN (0.01 M). This study was done by B. Pucci from the laboratory of *Chimie Bioorganique et des Systèmes Moléculaires Vectoriels (Université d'Avignon et des Pays de. Vaucluse, Faculté des Sciences, 33 rue Louis Pasteur, 84000 Avignon, France)*.
24 G. M. Rosen, L. D. Haire, G. A. Coulter, H. J. Stonks, P. H. Krygsman, R. A. Towner and J. W. Hilborn, *J. Org. Chem.*, 1989, **54**, 2915–2920.
25 C. Reichardt and E. Harbusch-Gôrnert, *Liebigs Ann. Chem.*, 1983, **5**, 721–743.
26 B. Halliwell, *Am. J. Med.*, 1991, **91**, 3C 14S–22S; B. Halliwell and J. M. C. Gutteridge, *Am. J. Med.*, 1984, **219**, 1–14; B. Halliwell and S. Chirico, *Am. J. Clin. Nutr.*, 1993, **57(S)**, 715S–725S.
27 R. Shridhar, P. C. Beaumont and E. L. Powers, *J. Radioanal. Nucl. Chem.*, 1986, **101**, 227–237; E. G. Janzen, R. D. Hinton and Y. Kotake, *Tetrahedron Lett.*, 1992, **33**, 1257–1260.
28 J. R. Harbour, V. Chow and J. R. Bolton, *Can. J. Chem.*, 1974, **52**, 3549–3553; E. G. Janzen, D. E. J. R. Nutter, E. R. Davis, B. J. Blackburn, J. L. Poyer and P. B. McCay, *Can. J. Chem.*, 1978, **56**, 2237–2242; C. E. Thomas, D. F. Ohlweiler, A. A. Carr, T. R. Nieduzak, D. A. Hay, G. Adams, R. Vaz and R. C. Bernotas, *J. Biol. Chem.*, 1996, **271**, 3097–3104.
29 M. M. Moccanu, S. E. Steare, M. C. W. Evans, J. H. Nugent and D. M. Yellon, *Free Radical Biol. Med.*, 1993, **15**, 459–463.
30 ROKI program: A. Rockenbauer and L. Korecz, *Appl. Magn. Reson.*, 1996, **10**, 29–48.
31 K. B. G. Torssell, *Nitrile Oxides, Nitrones and Nitronates in Organic Synthesis*, ed. H. Feuer, in *Organic Nitrochemistry Series*, VCH publishers, Inc, 1988, New York, p. 75–93.
32 Y. Kotake and E. G. Janzen, *J. Am. Chem. Soc.*, 1991, **113**, 9503–9506.
33 R. Lauricella, Daphnis program, Université de Provence, Marseille, France, 1997.
34 E. G. Janzen, Y. Kotake and H. D. Hinton, *Free. Radical Biol. Med.*, 1992, **12**, 169–173.
35 B. C. Gilbert, D. M. King and C. B. Thomas, *J. Chem. Soc., Perkin Trans. 2*, 1981, 1186–1199.
36 H. S. Isbell and H. L. Frush, *Carbohydr. Res.*, 1987, **161**, 181–193; H. S. Isbell and H. L. Frush, *Carbohydr. Res.*, 1987, **161**, 181–193; H. S. Isbell and P. Czubarow, *Carbohydr. Res.*, 1990, **203**, 287–289.
37 R. A. Floyd, K. Hensley, M. L. Forster, J. A. Kelleher-Andersson and P. L. Wood, *Mech. Ageing Dev.*, 2002, **123**, 1021–1023.